OPEN ACCESS

Scholars International Journal of Chemistry and Material Sciences

Abbreviated Key Title: Sch Int J Chem Mater Sci
ISSN 2616-8669 (Print) |ISSN 2617-6556 (Online)
Scholars Middle East Publishers, Dubai, United Arab Emirates
Journal homepage: http://saudijournals.com

Original Research Article

Effect of Sulfurization Temperature on the Chemical Composition and Phase Transformation of $CuAlS_2$ Thin Films Prepared by two-stage Vacuum Thermal Evaporation

B. A. Maiyama[1], S. Abdullahi[2*], A. M. Wara[1]

[1]Department of Science Technology, Waziri Umaru Federal Polytechnic Birnin Kebbi, Kebbi State Nigeria
[2]Department of Physics, Usmanu Danfodiyo University Sokoto, Nigeria

DOI: https://doi.org/10.36348/sijcms.2025.v08i02.007 | **Received:** 26.02.2025 | **Accepted:** 04.04.2025 | **Published:** 09.04.2025

***Corresponding author:** S. Abdullahi
Department of Physics, Usmanu Danfodiyo University Sokoto, Nigeria

Abstract

The study examined the effect of sulfurization temperature on chemical composition, structural properties and morphological features of $CuAlS_2$ thin films that had been prepared using two – step Vacuum Thermal Evaporation Technique. It was reported that metallic Cu – Al precursor layer first deposited onto soda – lime glass substrates before they were sulfurized and annealed at 573K, 673K, and 773K. The thin films were then characterized by X – ray Diffraction (XRD), Scanning Electron Microscopy (SEM), and Energy Dispersive X – ray Spectroscopy (EDS) to study their crystallographic phase, surface morphology and elemental composition respectively. XRD study disclosed the formation of a chalcopyrite tetragonal $CuAlS_2$ phase with notable variations of crystallinity and lattice parameters as a function of temperature. SEM images revealed that the film morphologies were influenced by sulfurization temperature and EDS analysis suggested non – ideal stoichiometry as a result of incomplete sulfurization at lower temperatures. Overall, the findings highlighted the crucial role of sulfurization temperature in determining material properties. The study also highlighted the potentials of $CuAlS_2$ thin films in optoelectronic devices, particularly solar cells and light- emitting diodes.

Keywords: Sulfurization, Annealing, Chalcogenide, Wide Band Gap, Abundant.

1. INTRODUCTION

Chalcopyrite materials with the formula $X^{I}Y^{III}Z_2^{VI}$ are ternary semiconductors which normally crystallize in chalcopyrite structure. It is a super lattice of the cubic zinc-blend structure, but the symmetry of the structure is lowered and, therefore, it is no longer cubic but tetragonal with the lattice parameters ratio (c/a) equal to or, in most cases, slightly less than 2. These materials have attracted a great deal of attention among various research groups because of their applications in solar cell, corrosion resistant coating, microelectronics, optics, magnetic, laser devices and gas sensor applications (Bhattacharyya *et al.*, 2018; Ahmed *et al.*, 2020).

$CuAlS_2$ (CAS) is a direct bandgap (3.5 eV) semiconductor at room temperature with large absorption coefficient, exciton binding energy and bond length (Brini *et al.*, 2009; Yu *et al.*, 2019; Shojaei *et al.*, 2021; Geng and Wu, 2023; Volniaska and Klopotowski, 2024) that belongs to the family of ternary chalcopyrite compounds. The crystal structure of ternary chalcopyrite has eight atoms per unit cell (Hossain *et al.*, 2024; Beggas *et al.*, 2024; Nascimento *et al.*, 2024). Each anion is tetrahedrally coordinated to two atoms of both cations, while each cation is coordinated to four anions. The Bravais lattice of chalcopyrite $CuAlS_2$ compound is body centered tetragonal unit cell possessing space group p 142d (No. 122) (Verma *et al.*, 2011; Nascimento *et al.*, 2024). At room temperature, the $CuAlS_2$ compound stabilized in the form chalcopyrite structure. Additionally, $CuAlS_2$ as a semiconductor has good luminescent properties making it suitable for use as material for light-emitting devices in the blue region of the spectrum (Brini *et al.*, 2009). This material is non-toxic, and its basic elements are abundant in nature (Chaki *et al.*, 2015).

The thin film of $CuAlS_2$ can be deposited using several methods such a but not limited to Dip coating (Chaki *et al.*, 2017), Hydrothermal (Sugan *et al.*, 2015), Chemical Bath Deposition Technique (Taher and

Ahmed, 2021), Chemical Vapour Transport (Srybu *et al.*, 2010), High Energy Mechanical Milling [Shojaei *et al.*, 2021], Chemical Spray Pyrolysis [Ahmad, 2017], Metal Organic Chemical Vapour Deposition (MOCVD) (Damisa *et al.*, 2017), Electrophoretic Deposition (EPD) (Guo *et al.*, 2016), Electron beam evaporation (Kawaguchi *et al.*, 2015) and Thermal Evaporation (Moreh *et al.*, 2013; Moreh *et al.*, 2014; Ata *et al.*, 2020; Hassan and Khudayer, 2020).

Here, the thermal evaporation method was chosen because of its cost effectives and simplicity for the preparation and deposition of $CuAlS_2$ thin films on soda lime glass substrates.

Experimental

2.1 Substrate Preparation

The corning glass substrates were thoroughly cleaned before the actual deposition of $CuAlS_2$ thin films. The cleaning process involves keeping the substrates in diluted chemical detergent at 100^{o}C for 10 minutes after which the substrates are rinsed with distilled water.

2.2 Growth of $CuAlS_2$ Thin Films

The first stage is to grow the precursor of Cu-Al using an EDWARDS FL 400 thermal evaporator equipped with SQC-310C deposition controller. Molybdenum boat was used as source for the deposition of copper and tungsten coil was used for the deposition of aluminum. The six (6) samples of Cu-Al films to be grown will be of different thicknesses (100 nm and 200 nm) that will be deposited at a substrate temperature of room temperature (RT) and 373K.

2.3 Sequential Deposition of the Cu-Al Precursor

A metallic precursor with Cu-Al bi-layer structure was prepared on glass substrate by vacuum thermal evaporation of 4N grade copper and aluminum in a sequential mode. As mentioned above, molybdenum boat was used as source for the deposition of copper and tungsten coils were used for deposition of aluminum.

2.4 Sulfurization/annealing of the Thin Films

This is the conversion of metallic Cu-Al thin films to $CuAlS_2$ thin films by reaction in sulfur vapor at a given temperature. This was carried out by annealing Cu-Al thin films in elemental sulfur at a temperature of 573K, 673K and 773K using a horizontal diffusion furnace (SVG SYSTEM 2610 BASE) which was equipped with an external mini sulfur furnace.

2.5 Characterization

The structural properties of the six (6) thin film samples were analyzed with the aid of X-Pert pro X-ray diffractometer with a scanning rate of 1 degree per minute and a wavelength (λ) of Cu K_α = 1.504Å. The XRD was also used to study the crystallinity of the film. EVO MA10 SEM was applied to observe the surface morphology (at a magnification of 5000 $\times$) and the elemental composition of the samples.

Figure 1 represents the flow chart of the thin film deposition (by two-stage vacuum thermal evaporation) and characterization.

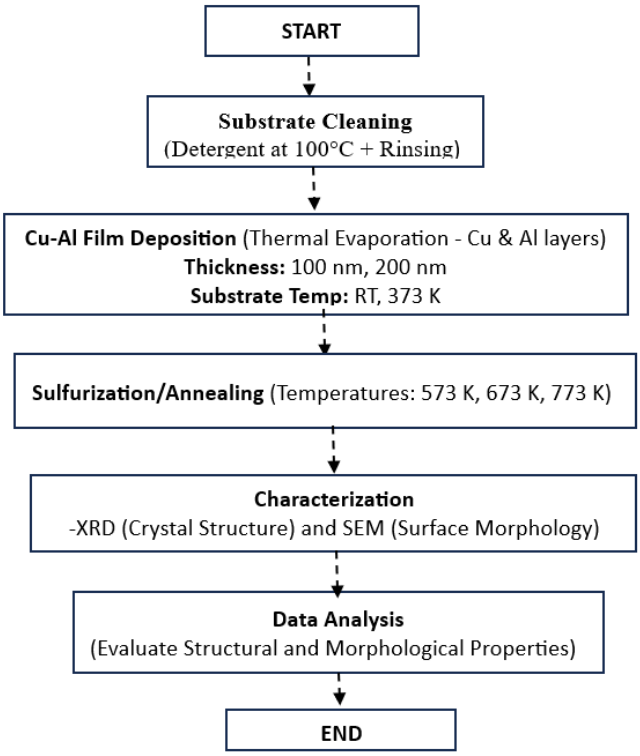

Figure 1: Flow chart of $CuAlS_2$ thin film deposition and characterization

3.0 RESULTS AND DISCUSSION

3.1 X-Ray Diffraction Analysis

The X-ray diffraction patterns of $CuAlS_2$ thin films with different thickness (100 nm and 200 nm) and sulfurized/annealed at different temperatures (573K, 673K and 773K) are displayed in Figures 2a and 2b. All the diffraction patterns of $CuAlS_2$ are indexed to the chalcopyrite tetragonal crystal structure. It is known that in the tetragonal crystal structure, each atom has four nearest neighbors, and each anion (S atom) is coordinated by four cations (two Cu and two Al atoms), whereas each cation is tetrahedrally surrounded by four anions. From two consecutive lattice planes, the term $2dsin\theta$ of the diffraction of X-rays for crystalline materials is given by Equation [1]

$$n\lambda = 2dsin\theta \quad (1)$$

Where n is the order of reflection (an integer), λ is the wavelength of the incident X-ray, d is the d-spacing and θ is the angle of diffraction.

The lattice constant values in Tetragonal system can be realized from Equation [2] given by (Hassan and Khudaye, 2020; More *et al.*, 2024).

$$\frac{1}{d^2} = \left(h^2 + \frac{k^2}{a^2}\right) + l^2/c^2 \quad (2)$$

The diffraction patterns are consistent with JCPDS no: 075-0100 for $CuAlS_2$ and 01-083-1574 for Chalcophyllite. In Figure 1a, the diffraction peaks for the sample of 100 nm thickness and sulfurized/annealed at 573K located at $2\theta = 29.59$, 38.13 and 77.61° corresponds to (112), (211), (200), (220) and (312) planes while those at $2\theta = 42.67$ and 48.00° corresponds to (200) and (220) chalcophyllite planes. For the sample sulfurized/annealed at 673K, the peaks are located at $2\theta = 30.93$, 64.27, 76.01 and 81.35° corresponding to (112), (204), (312) and (204) of $CuAlS_2$. The diffraction angles and the plane of the sample sulfurized/annealed at 773K are $2\theta = 29.06$, 31.19, 52.27, 62.94 and 74.14° are indexed at (112), (101), (220), (116) and (400) respectively. Figure 1b displays the XRD of the samples of 200 nm thicknesses and sulfurized/annealed at 573K, 673K and 773K each samples bear four peaks. The peaks at $2\theta = 29.71$, 38.52, 68.93 and 73.73° corresponding to (112), (211), (312) and (213) belong to the sample sulfurized/annealed at 573K. The sample sulfurized/annealed at 673K is having $2\theta = 28.92$, 30.79, 64.39 and 81.20° indexed at (112), (103), (204) and (224) for $CuAlS_2$. In the sample sulfurized/annealed at 773K, the peaks at $2\theta = 29.10$, 47.77, 59.24 and 82.98° corresponds to (112), (220), (303) and (314) plane of CuAlS2. The weak peaks (220) are attributed to the presence of Al-Cu alloys (Ghrib *et al.*, 2013).

Other unidentified peaks may belong to compounds such as CuAlO2, CuAl, CuS2 and Cu2O (Ahmad, 2017; Ata *et al.*, 2020; More *et al.*, 2024).

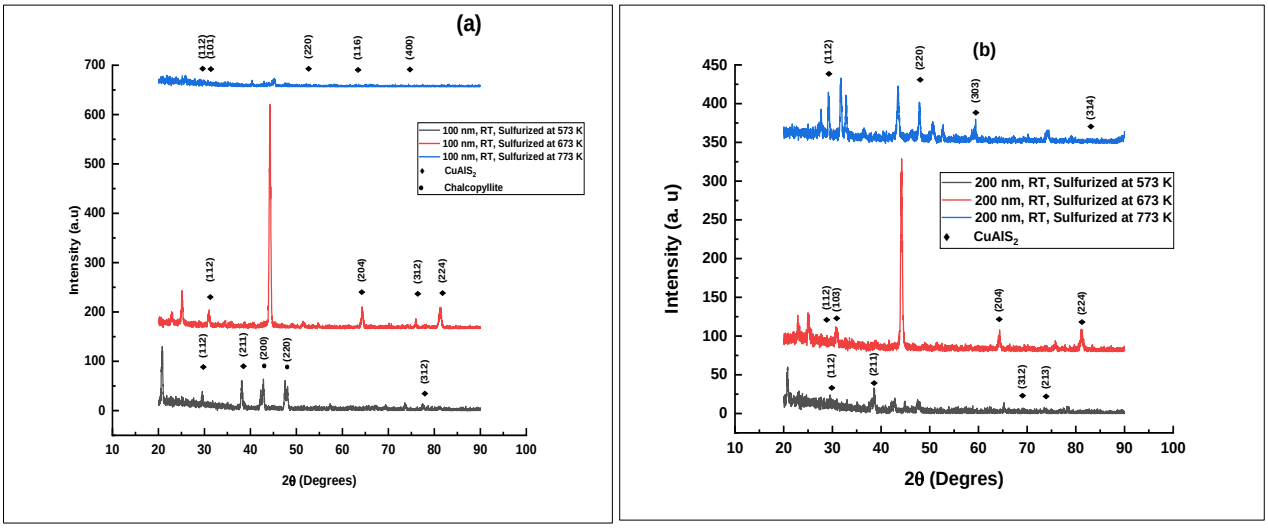

Figure 2: XRD patterns of $CuAlS_2$ thin films of 100 nm (a) and 200 nm (b) thickness and sulfurized/annealed at 573K, 673K and 773K

Table 1 shows Film thickness, Sulfurization temperature, Diffraction angle (2θ), Full Width at Half Maximum (FWHM), d-spacing, Dislocation Density, Crystalline per unit Surface (N), Crystallite Size (D), Residual Stress, Specific Surface Area (SSA) and the Microstrain calculated from the (112) reflection/plane of the CuAlS2 thi film samples of 100nm and 200nm sulfurized/annealed at 573K, 673K and 773k.

The d-spacing and can be computed from Equation [3] given by (Muthee *et al.*, 2021)

$$d = \frac{\lambda}{2\ sin\theta} \quad (3)$$

Wher λ=0.154nm (Cu Kα X-ray wavelength) and $\theta = \frac{2\theta}{2}$

Dislocation Density has been defined as Equation [4] by Edalati and Enikeev (2024) and (Laske *et al.*, 2023) as;

$$\delta = \frac{1}{D^2} \quad (4)$$

Where D is the crystallite size

Using Scherrer Equation given as Equation [6] from Dahivade *et al.,* (2024) the crystallite size can be determined.

$$D = \frac{0.9\lambda}{\beta cos\theta} \quad (6)$$

Where β represents the full width at half maximum, λ is the X-ray wavelength (1.506 Å), while θ is the diffraction angle.

Crystallites per unit area (N) was estimated by using Equation [7], by Hashemi *et al.,* (2022)

$$N = \frac{t}{d^3} \quad (7)$$

Where d is the d-spacing and t the film's thickness

The specific surface area of the samples was calculated from Equation [8], by (Lyson-Sypien *et al.*, 2015).

$$SSA = \frac{6}{D.\rho} \quad (8)$$

Where ρ =3.53 Mg/m^3 (density of $CuAlS_2$).

For the 100 nm sample anneled at 573K, $2\theta = 29.59°$, the FWHM is comparatively large at 0.4723, suggesting a sharper peak, which often corresponds to larger crystallite size or lower strain (Chaki *et al.,* 2015), also indicating well-formed crystals. For the 100 nm thick samples annealed at 673K and 773K, the FWHM decreased to 0.0704 and 0.0562 respectively. For the 200 nm thick samples annealed at 573K, 673K and 773K, the FWHM varies. It has been reported in the literature that a lower FWHM value corresponds to larger crystallite size (Olgar *et al.,* 2021).

The d-spacing is the distance between adjacent planes of atoms in a crystal lattice. This parameter therefore influences the angles at which X-rays are diffracted when interacting with the crystal. The relationship between d-spacing and the diffraction angle is described by Equation [1], which is the Bragg's Law. From table 1, the d-spacing of the 100 nm samples annealed at various sulfurization/annealing temperatures decreases with increase in the annealing temperature while that of the 200 nm thick samples varies. The dislocation density of all the samples is also presented in table 1. Dislocation in a crystal shows defects or disorders that influence the physical and chemical properties of the crystal (Hajiabadi *et al.,* 2019). Variations in the dislocation density are related to stress relaxation, which occurs during the recrystallization process (Hashemi *et al*., 2022). It has also been reported (Caglar *et al*., 2008) that decrease in dislocation density is related to the reduction in the concentration of lattice imperfections. The crystalline per unit surface slightly varies with the sulfurization/annealing temperature for all the samples. Variation has also been observed for the grain size (D). Increased grain size is indicative of an enhancement in the 2D in-plane growth mode of a material (Qiu *et al.,* 2024). The residual stress of all the samples is compressive being negative (Laska *et al.,* 2023). This means that the films lattice is compressed relative to its natural state. This behavior is related to thermal mismatch between the substrate and film during deposition, lattice mismatch at the interface or growth-induced strain from high deposition rates or non-equilibrium conditions.

This may lead to the enhancement of adhesion between the film and substrate or may improve mechanical stability. Generally, compressive stress can cause potential defects (e.g., buckling or delamination) if the stress exceeds a critical limit.

However, these samples have the potential to be applied to surfaces requiring dense, well-adhered films (e.g., optical coatings or barrier layers).

The micro – strain of the samples, 100 nm samples decreases with increase in sulfurization/ annealing temperature. High micro – strain may be related to inclusion of dissimilar materials in symmetry (Jayaram *et al.,* 2016).

Table 1: Some of the important sructural parameters of $CuAlS_2$ thin films deposited by two stage thermal evaporation

Thickness/Sulfurization Temperature	2θ (112)	FWHM (Degrees)	D-spacing (nm)	Dislocation Density (line/m^2)$\times 10^{15}$	Crystalline per Unit Surface (N) ($m^{-2} \times 10^{12}$)	Grain Size (D) (nm)	Residual stress	Specific Surface Area ($m^2 g^{-1}$)	Micro - strain (ε)
100nm/573K	29.59	0.4723	2.97381	10.8574	0.0380	0.3035	-45.06	4.39	0.4506
100nm/ 673K	30.93	0.0787	3.02525	0.2988	0.0361	1.8293	-7.04	0.73	0.0704
100nm/ 773K	29.06	0.059	3.05102	0.1696	0.0352	2.4282	-5.67	0.55	0.0567
200nm/ 573K	29.71	0.072	3.03697	0.2518	0.0357	1.9929	-6.76	0.67	0.0676
200nm/ 673K	28.92	0.09	3.0431	0.3945	0.0355	1.5922	-8.63	0.84	0.0863
200nm/ 773K	29.10	0.072	3.01625	0.2526	0.0364	1.9899	-6.92	0.67	0.0692

3.2 Morphological Studies

Plate 1 represents the SEM surface images of $CuAlS_2$ thin films of 100 nm and 200 nm thickness sulfurized / annealed at different temperatures. As shown in the surface images, the sample sulfurized / annealed at 573K (a) shows rough surface with large grains. However, samples sulfurized /annealed at 673K become more crystalline with larger grains. The sample sulfurized /annealed at 773K also of 100 nm thickness shows a cloudy and non – uniform surface.

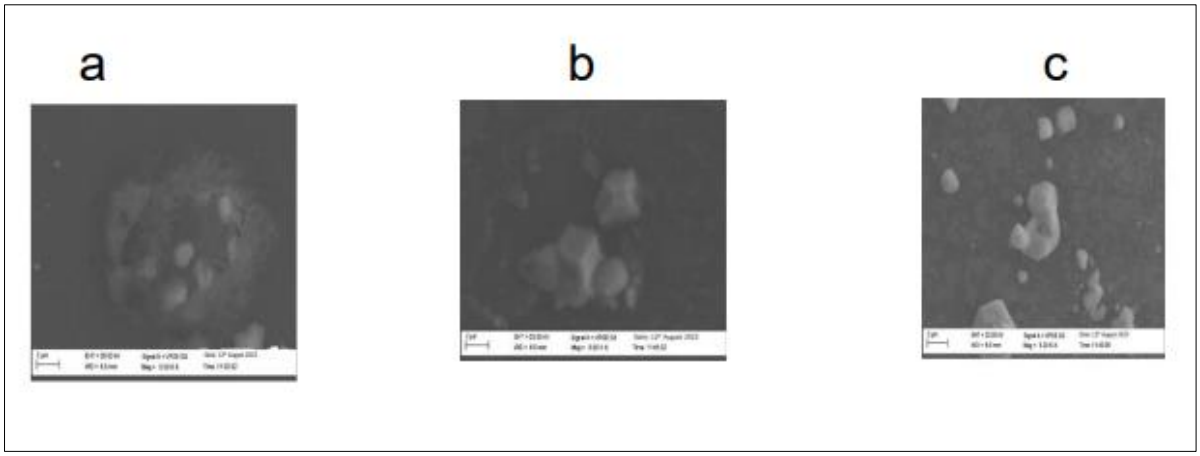

Plate 1: SEM surface images of $CuAlS_2$ thin films of 100nm sulfurized/annealed at 573 (a), 673 (b) and 773K (c)

Plate 2 represents the 200 nm sample sulfurized/annealed at 573K that shows flake-like structure (a) which may be because of the presence of aluminum particles. As the temperature increased to 673K the flake-like structure completely disappeared (b). Sample (c) appeared cloudy with no grain boundaries.

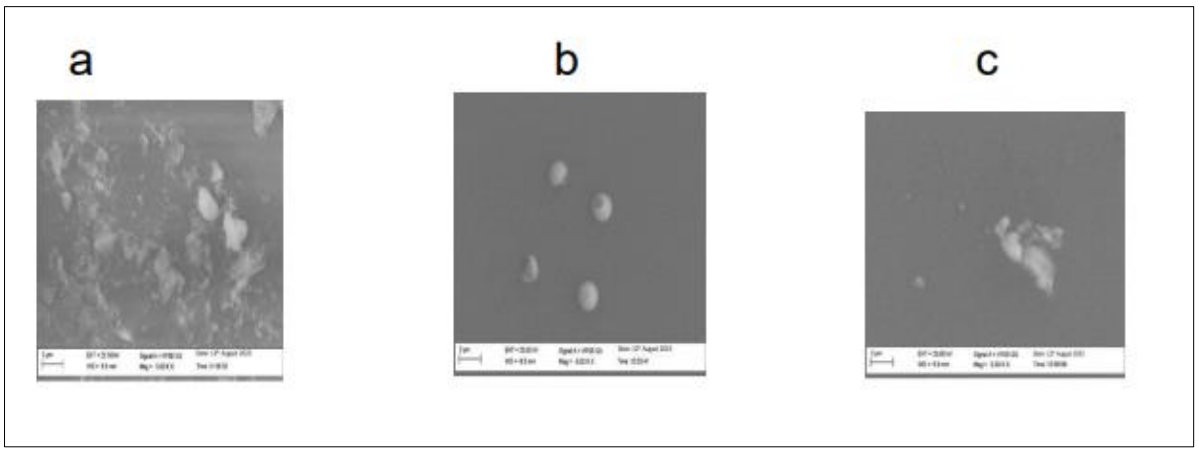

Plate 2: SEM surface images of $CuAlS_2$ thin films of 200nm sulfurized/annealed at 573 (a), 673 (b) and 773K (c)

Table 2 shows the average atomic % taken at three different spots on each $CuAlS_2$ thin film sample. As reported in the literature, atomic % represents the proportion of atoms, which is relevant for studying stoichiometry. Here, aluminum is taken as the reference (set to 1). For a compound like $CuAlS_2$, the ideal stoichiometry should be 1:1:2, meaning for every 1 atom of Cu, there should be 1 atom of Al and 2 atoms of S. The purpose of this ratio calculation is to check how close each sample is to ideal stoichiometry. For the 100nm thick sample annealed at 573K, copper is close to the expected value while sulfur is much lower than expected. This sample may not exhibit proper $CuAlS_2$ characteristics. At a sulfurization/annealing temperature of 673K, the alumimum and the sulfur content has increased.

Lower values of sulfur may indicate incomplete sulfurization of the samples. The 100nm sample annealed at 773K, exhibited higher aluminum and sulfur content. The aluninum and sulfur content of the 200nm samples shows no improvement except for the sample sulfurized/annealed at 573K in which the copper and the sulfur content is far greater from the stoichiometry. Decrease observed in the ammount of sulfur in all the samples may be as a result of evaporation of certain ammount of sulfur due to the annealing process (Ahmed *et al.*, 2020).

Table 2: Atomic percentages of $CuAlS_2$ thin films

Sample	Cu (at %)	Al (at %)	S (at %)	Cu/Al (at %)	S/Al	Ratio
100nm/573K	3.70	4.10	0.27	0.90	0.07	0.9:1:0.07
100nm/673k	4.89	2.52	0.28	1.94	0.11	1.94:1:0.11
100nm/773K	4.59	1.51	2.94	3.04	1.94	3.04:1:1.94
200nm/573K	7.86	0.73	3.67	10.70	5.03	10.7:1:5.03
200nm/673k	16.05	13.01	0	1.23	0	1.23:1:0
200nm/773K	19.14	7.21	0	2.65	0	2.65:1:0

CONCLUSION

The influence of sulfurization temperature on the chemical composition, crystallographic structure, and morphology of $CuAlS_2$ thin films, prepared by a two-stage vacuum thermal evaporation method, was investigated. Sulfurization/annealing temperatures of 573K, 673K, and 773K were applied, and the structural, morphological, and chemical properties of the thin films were studied using XRD, SEM, and EDS. The results indicated that sulfurization temperature is an important factor in deciding the structural and morphological characteristics of the thin films.

At 673K, the films presented the best crystallinity, with well-identified chalcopyrite $CuAlS_2$ phases and few defects. SEM characterization showed better surface homogeneity and bigger grains at this temperature compared to the others. The EDS analysis pointed out deviations from ideal stoichiometry, mainly for lower and higher temperatures, where incomplete sulfurization and loss of sulfur were observed.

In summary, a sulfurization temperature of 673K is suggested for $CuAlS_2$ thin film growth with improved structural and morphological properties. These results can be regarded as a guideline for further improvement in $CuAlS_2$ thin films for their applications in solar cells, photodetectors, and light-emitting devices.

Credit Authorship Contribution Statement

Buhari Abdullahi Maiyama: Funding acquisition, Supervision, Investigation, Resources.
Sanusi Abdullahi: Conceptualization, Data curation, Writing – original draft, Validation
Aliyu Muhammad Wara: Project administration, review and editing

Declaration of Competing Interest

The authors declare that they have no known competing interests that could have appeared to influence the work reported in this communication.

Acknowledgements

The authors would like to thank the Tertiary Education Trust Fund (tetfund) through the Waziri Ummaru Federal Polytechnic Birnin Kebbi, Kebbi State Nigeria for sponsoring this research.

REFERENCES

- Ahmad, S. M (2017). Study of the optical properties of CuAlS2 thin films prepared by two methods. Appl. Phys. A, 123, 1-9. DOI 10.1007/s00339-017-0833-5
- Ahmed, E. A, Ata, M. H., Mohammed, M. E & Ali, H. M (2020). Study the effect of the Sintering Temperature on the Microstructure and optical reflectance of the compacted bulk CuAlS2 fabricated by Powder Metallurgy Technique (P/M). European Journal of Mechanical Engineering Research, 7 (2), 5-13
- Ata, M. H., Abdellateef, E & Elrouby, M (2020). Chalcopyrite CuAlS2 nanocomposite thin films with unusual and promising peculiarities fabricated by two consecutive methods; powder metallurgy and thermal evaporation, Materials Science and Engineering: B, 261, 114688, doi: 10.1016/j.mseb.2020.114688.
- Beggas, K., Boucerredj, N and Ghemid, S (2024). Structural electronic and optical properties of chalcopyrite compound $AuMTe_2$ (M = Ga, In) from first-principles calculation. *Indian J Phys* 98, 2755–2774. https://doi.org/10.1007/s12648-023-03049-4
- Bhattacharyya, B., Pandit, T., Rajasekar, G. P and Pandey, A (2018). Optical Transparency Enabled by Anomalous Stokes Shift in Visible Light-Emitting $CuAlS_2$-Based Quantum Dots. Journal of Physical Chemistry Letters. 9 (15), 4451.
- Brini a, R., Schmerber, G., Kanzari, M., Werckmann, J and Rezig, B (2009). Study of the growth of CuAlS2 thin films on oriented silicon (111). Thin Solid Films 517, 2191–2194. Chaki, S. H.,
- Caglar, M., Ilican, S & Caglar, Y (2008). Structural, morphological and optical properties of CuAlS2 films deposited by spray pyrolysis method. Optics Communications 281 (2008) 1615–1624
- Chaki, S. H., Mahato, K. S and Deshpande, M. P (2015). Catalytic action of CuAlS2 microparticles and nanoparticles in cellulose pyrolysis. Phys. Scr. 90, 1-12. doi:10.1088/0031-8949/90/4/045701
- Chaki, S. H., Mahato, K. S., Malek, T. J & Deshpande, M (2017). CuAlS2 thin films–Dip coating deposition and characterization, J. Sci. Adv. Mater. Devices 2 (2017) 215–224, https://doi.org/10.1016/j.jsamd.2017.04.002.
- Dahivade, P. B., Randive, S. G., Fugare, B. Y., Sathe, V. S., Thakur, A. V & Lokhande, B. J (2024). Nano-crystalline Cadmium Oxide Thin Films for

Supercapacitor Application: Effect of Solution Concentrations. ES Energy Environ., 2024, 23, 1105. DOI: https://dx.doi.org/10.30919/esee1105

- Damisa, J., Olofinjana, B., Ebomwonyi, O., Bakare, F and Azi, S. O (2017). Morphological and optical study of thin films of CuAlS2 deposited by metal organic chemical vapour deposition techniqueMaterials Research Express 4(8), 086412
- Edalati, K and Enikeev, N (2024). Dislocation Density in Ceramics Processed by Severe Plastic Deformation via High-Pressure Torsion. *Materials* 2024, *17* (24), 6189; https://doi.org/10.3390/ma17246189
- Geng, J and Wu, J (2023). Effects of pressure on structural, mechanical, and electronic properties of chalcopyrite compound CuAlS2. Chalcogenide Letters, 20 (3), 215 – 225.
- Ghrib, T., Brini, R., Al-otaibi, A. L & Al-messiere, M. A (2013). Thermal and Structural Study of Mono- and Multi-Layered Thin Films Composed of CuAlS2 Chalcogenide. CHIN. PHYS. LETT. 30 (10) 1085031-4
- Guo, C., Yang, C., Xie, Y., Chen, P., Qin, M., Huang, R & Huang, F (2016). Preparation of Sn-doped $CuAlS_2$ films with an intermediate band and wide-spectrum solar response. RSC Advances 6(47), 40806.
- Hajiabadi, M. G., Zamanian, M and Souri, D (2019). Williamson-Hall analysis in evaluation of lattice strain and the density of lattice dislocation for nanometer scaled ZnSe and ZnSe: Cu particles. Ceramics International 45, 14084-14089. https://doi.org/10.1016/j.ceramint.2019.04.107
- Hashemi, M., Saki, Z., Dehghani, M. *et al.* Effect of transparent substrate on properties of $CuInSe_2$ thin films prepared by chemical spray pyrolysis. *Sci Rep* 12, 14715 (2022). https://doi.org/10.1038/s41598-022-18579-w
- Hassan, N. and Khudayer (2020). Thickness Effect of CuAlTe2 Thin Films on Morphological, Structural and Visual Properties. Ibn Al-Haitham Journal for Pure & Applied Science, 33 (3), 27-43
- Hossain, A., Ali, M. A., Uddin, M. M., Naqib, S. H and Hossai, M .M (2024). Theoretical studies on phase stability, electronic, optical, mechanical and thermal properties of chalcopyrite semiconductors $HgXN_2$ (X=Si, Ge and Sn): A comprehensive DFT analysis. Materials Science in Semiconductor Processing. 172, 108092
- Jayaram, P., Pradyumnan, P. P and Karazhanov, S. Zh (20216). Microstrain, dislocation density and surface chemical state analysis of multication thin films, Physica B: Physics of Condensed Matter, 501, 140-145. http://dx.doi.org/10.1016/j.physb.2016.08.018
- Kawaguchi, H., Ishigaki, T., Adachi, T., Oshima, Y and Ohmi, K (2015). Si-co-doped $CuAlS_2$: Mn conductive phosphor thin films prepared by electron beam evaporation using phosphor powder pellets**.** Physica Status Solidi C Current Topics in Solid State Physics 12(6), 793.
- Laska, A., Szkodo, M and Cavaliere, P (2023). Analysis of Residual Stresses and Dislocation Density of AA6082 Butt Welds Produced by Friction Sir Welding. *Metall Mater Trans A* 54, 211–225. https://doi.org/10.1007/s11661-022-06862-4
- Lyson-Sypiena, B., Radecka, M., Rekas, M., Swierczek, K., Michalow-Mauke, K., Graulee, T and Zakrzewska, K (2015). Grain-size-dependent gas-sensing properties of TiO2 nanomaterials. Sensors and Actuators B, 211, 67–76
- Mahato, K. S and Deshpande, M. P (2015). Catalytic action of CuAlS2 microparticles and nanoparticles in cellulose pyrolysis. Phys. Scr. 90, 1-12. doi:10.1088/0031-8949/90/4/045701
- More, S. G., Parveen, F., Pathan, H. M., Jadkar, S. R and Gadakh, S. R (2024). Biomolecule-assisted Hydrothermal Synthesis of Copper Aluminium Sulfide: Application for Dye Degradation, ES Energy & Environment, 25, 1-11
- Moreh, A. U., Momoh, M., Hamza, B., Abdullahi, S., H. N. Yahya, S. Namadi & S. Umar. (2013). Influence of Substrate Temperature on Electrical Resistivity and Surface Morphology of $CuAlS_2$ Thin Films Prepared by Vacuum Thermal Evaporation Method. *International Journal of Nano and Material Sciences*, 3(1) 47-55. ISSN: 2166-0182 (online).
- Moreh, A. U., Momoh, M., Yahya, H. N., Hamza, B., I. G. Saidu and S. Abdullahi (2014). Effect of Thickness on Structural and Electrical Properties of $CuAlS_2$ Thin Films Grown by Two Stage Vacuum Thermal Evaporation Technique, World Academy of Science, Engineering and Technology *International Journal of Physical and Mathematical Sciences*, 8 (7), 1084-1088. ISNI:0000000091950263
- Nascimento, G. R., Bazan, S. F and de Lima, G. F (2024). A brief review on computer simulations of chalcopyrite surfaces: structure and reactivity. Crystallography in Latin America, 80(9), 458-471. https://doi.org/10.1107/S2053229624006867
- Olgar, M. A., Basol, B. M., Tomakin, M and Bacaksız, E (2021). Phase transformation in Cu2SnS3 (CTS) thin films through pre-treatment in sulfur atmosphere. J Mater Sci: Mater Electron (2021) 32:10018-10027. https://doi.org/10.1007/s10854-021-05660-9
- Qiu, F., Deng, W., Shi, X., Ai, D., Ren, X., Dong, A., Zhang, X and Jie, J (2024). Large-Area Deposition of Highly Crystalline F4-Tetracyanoquinodimethane Thin Films by Molecular Step Templates. Small Sci. 2024, 4, 2400038. DOI: 10.1002/smsc.202400038
- Shojaei, M., Shokuhfar, A and Zolriasatein, A (2021). Synthesis and characterization of CuAlS2

nanoparticles by mechanical milling. Materials Today Communications 27 (2021) 102243

- Sugan, S., Baskar, K and Dhanasekaran, R (2015). Structural, morphological and optical studies on CuAlS2 and CuAlSe2 nanorods prepared by hydrothermal method, J. Alloys. Compd. 645 (2015) 85–89, https://doi.org/10.1016/j.jallcom.2015.04.129
- Volnianska, O and Kłopotowski, L (2024). Effect of Cation Cu/Al Ratio and Surface Proximity on the Electronic Structure and Optical Properties of Cu-Rich Cu1+xAl1−xS2−y: A DFT Study. J. Phys. Chem. C 2024, 128, 18039−18050. https://doi.org/10.1021/acs.jpcc.4c03712
- Yu, Y., Kong, X. G., Shen, Y. H and Deng, J (2019). Thermodynamic Properties of CuAlS2 with Chalcopyrite Structure from First-principles Calculations. Chalcogenide Letters, 16 (11), 513 - 522